Turk Neurosurg 34(2):184-195, 2024

Original Investigation

DOI: 10.5137/1019-5149.JTN.21876-17.5

Received: 18.10.2017
Accepted: 30.06.2018

Published Online: 05.11.2018

Identification of Driver Genes and Key Pathways of Ependymoma

Sheng ZHONG[1,2], Qi YAN[3], Junliang GE[2], Gaojing DOU[2], Haiyang XU[1], Gang ZHAO[1]

[1]The First Hospital of Jilin University, Department of Neurosurgery, Changchun, China
[2]Jilin University, Clinical College, Changchun, China
[3]Qiqihar Medical University, Clinical College, Qiqihar, China

Corresponding author: Gang ZHAO, Haiyang XU ✉ zhaogang_jdyy@126.com, xuhaiyang76@163.com

ABSTRACT

AIM: To identify ependymoma (EPN) driver genes and key pathways, and also to illuminate the connection between prognosis of EPN patients and expression levels of driver genes.

MATERIAL and METHODS: The gene expression profiles of GSE50161, GSE66354, GSE74195, and GSE86574 were analyzed to figure out the differentially expressed genes (DEGs) between tissue of EPN and normal brain samples. To harvest the enrichment functions, pathways and hub genes, the Gene ontology (GO), Kyoto Encyclopedia of Genes and Genomes (KEGG) analysis, and protein-protein interaction (PPI) network analysis were made. Subsquently, survival analysis was performed in 325 patients to illuminate the connection between prognosis of EPN and expression levels of hub genes.

RESULTS: 20 functions and 10 pathways which were up- or downregulated between the EPN and normal samples were revealed applying GO and KEGG analysis. Mutual hub genes were TP53, TOP2A, CDK1, PCNA, and ACTA2. The pathways of Hedgehog and notch signaling, mismatch repair (MMR), and retrograde endocannabinoid were significantly abnormally regulated in EPN tissue. Survival analysis revealed favorable progression-free (PFS) and overall (OS) survival in EPN patients with low expression of TOP2A, CDK1, PCNA, and ACTA2 ($p<0.05$).

CONCLUSION: Patients with lower expression of TOP2A, CDK1, PCNA, and ACTA2 had a longer OS and PFS. The differential expressed genes identified and the key pathways selected in this research provided unprecedented and promising targets for diagnosis and treatment of EPN patients.

KEYWORDS: Bioinformatics, Brain science, Ependymoma, Pathway, Target therapy

INTRODUCTION

Ependymoma (EPN) is the third most common pediatric brain tumor, accounting for 2–9% of all neuroepithelial tumors and for 6–12% of intracranial tumors in children (23,29). This slow-growing tumor occurs in all age bracket without sex preference. However, there are location and histological type preferences during the EPN formation process. Ependymoma can develop at any site along the neuroaxis, especially in the posterior fossa, supratentorium, and spinal cord. Infratentorial EPNs are more common in children, while spinal EPNs usually occur in adults (15). On the basis of the 2016 World Health Organization (WHO) central nervous system (CNS) classification, EPN includes three histopathological variants: papillary (PE); clear-cell (CCE); and tanycytic (TE) EPN (16). This classification of EPN and grading scheme is more accurate and systematic than its 2007 predecessor in its clinical use, whereas an urgent need remains for neurosurgeons and neurologists to explore the underlying oncogenesis mechanism of EPN. The main treatment regarding EPNs is surgical resection. After tumor resection and subsequent radiotherapy, patients usually have a 70% or greater likelihood

Sheng ZHONG : 0000-0002-2853-6347
Qi YAN : 0000-0001-6091-4208
Junliang GE : 0000-0003-0061-1437
Gaojing DOU : 0000-0003-0446-4411
Gang ZHAO : 0000-0002-0285-120X

of long-term survival (18). However, therapeutic results were not optimistic when intraoperative monitoring potentials fell below 50% or if more than three spinal segments have been occupied by tumor (22). Meanwhile, there is no clear description of the neoplastic processes of EPN. Therefore, studies that comprehensively depict molecular pathogenesis of EPN as well as identify novel therapeutic targets for EPN are necessary and crucial, not only to improve our understanding regarding the existing WHO 2016 molecular classification of EPNs, but also to help establish new grading schemes in the future.

The *C11orf95-RELA* fusion gene has been reported to be the driver factor of EPN oncogenesis, along with nuclear factor-κB (NF-κB), miR-124-3p, and TP53INP1, which all contribute to EPN occurrence and development. Potentially, they could be therapeutic targets for EPN in the future (6,17). However, few specific driver genes have been proved to be related to EPN pathogenesis. The connection between prognosis of EPN patients and expression levels of certain genes was not clear according to previous investegation. Knowledge regarding EPN remains superficial and provincial, therefore more oncogenesis mechanisms of EPN must be further investigated and illustrated (33). Therefore, exploring the molecular pathogenesis inculding proliferation, migration, and metastasis of EPN are urgently needed (9).

Bioinformatics methods, particularly united with microarray technology, raised a novel strategy to determine the molecular mechanisms of illness, especially tumors (35). We used these methods, especially through molecular data mining, combined with gene ontology (GO), Kyoto Encyclopedia of Genes and Genomes (KEGG) analysis, and protein-protein interaction (PPI) network analysis, employing four mRNA microarray datasets (GSE50161, GSE66354, GSE74195, and GSE86574) to locate the differentially expressed genes (DEGs) and hub genes as well as key pathways associated with EPN. By comparing gene expression levels of EPN to those of normal tissues, we provided four potential targets for further researches of molecular mechanisms, and identified the abnormal regulated signal pathway of EPN. Our conclusion was verified in the following real-time quantitative reverse transcription-polymerase chain reaction (RT-qPCR) assays and survival analysis. Meanwhile, we clarified the EPN developing process at the molecular level. The framework of this study is shown in Figure 1.

MATERIAL and METHODS

This study was approved by the Ethics Committee of the First Hospital of Jilin University.

Microarray data

The four mRNA microarray datasets (GSE50161, GSE66354, GSE74195, and GSE86574) were based on the Agilent GPL570 platform ((HG-U133_Plus_2) Affymetrix Human Genome U133 Plus 2.0 Array; Agilent Technologies, Santa Clara, CA, USA). GSE86574 has 39 and 10, GSE74195 has 14 and five, GSE66354 has 83 and 13, and GSE50161 has 46 and 13 EPN and normal samples, respectively. The samples were obtained from the Department of Pediatrics, University of Colorado Denver (GSE50161, GSE66354, and GSE86574; Denver, CO, USA), and the Erasmus Medical Center (GSE74195; Rotterdam, The Netherlands).

Identification of DEGs

Primary data files of these datasets were supplied as TXT files. GeneSpring software (version 11.5, Aglient) was used to analyze the data. All data were classified as two groups (EPN and CON) according to the EPN and control groups. We compared two groups from the same dataset to locate the DEGs between EPN and normal cells. The probe quality control of software Genespring was determined based on hierarchical clustering analysis and principal component. Probes with intensity values below the 20th percentile were weeded out using the "filter probesets by expression" option. The location of DEGs was achieved by applying a classical *t*-test with a change >2-fold, meanwhile statistical significant was defined as a p-value cut off of <0.01. Based on the four mRNA microarray datasets, we operated this analysis four times (GSE50161, GSE66354, GSE74195, and GSE86574). After that, website instrument (http://bioinformatics.psb.ugent.be/webtools/Venn/) was used to conduct analysis of Venn plot about the DEGs located form four groups.

GO, pathway enrichment, and Gene Set Enrichment Analysis (GSEA) of DEGs

An online program called The Database for Annotation, Visualization and Integrated Discovery (DAVID, http://david.abcc.ncifcrf.gov/) was applied to provide an integrated set of functional annotation tools to comprehended the biological significances underlying genes. GO and KEGG pathway enrichment analysis was operated by pooling the located DEGs into the DAVID database. This study considers p<0.05 as a significant difference. To obtain the differential expression genes with more clinical significance, results of GO and KEGG enrichment about four groups and Venn plot were analyzed. GSEA software was used to analyze DEGs to determine significantly abnormal regulated KEGG pathways.

PPI network analysis and modules selection

Recent years, the Search Tool for the Retrieval of Interacting Genes (STRING, http://string.embl.de/) database was applied for the construction of DEGs' PPI network. The modules with degree scores >62 and number of nodes >9 was screened using The Molecular Complex Detection (MCODE) base on Cytoscape software. Then, DEGs belong to modules were selected for GO and KEGG analysis to locate their enrichment functions and pathways. This study considers significant difference with $p<0.05$.

Cell lines

HEB (Human glial cells) and EPN cell lines (BXD-1425EPN, DKFZ-EP1NS, R254) were given. These cells were cultured in Dulbecco's Modified Eagle's medium (DMEM; Hyclone, Logan, UT, USA) mixing with 10% fetal bovine serum (FBS; Gibco Laboratories, Gaithrsburg, MD, USA). A moist environment

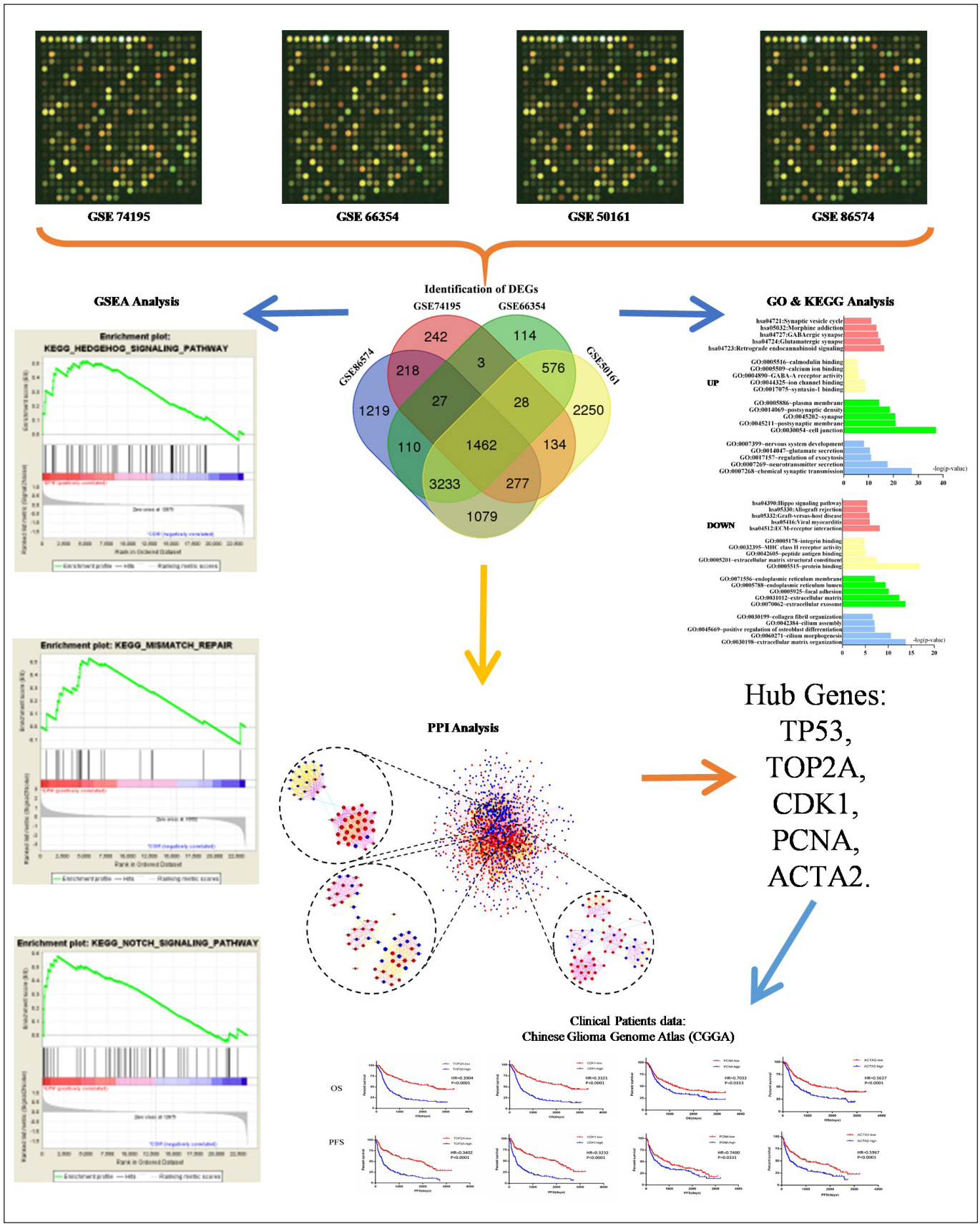

Figure 1: Framework of this study.

was constructed with 5% CO_2, 95% air, as well as proper temperature (37 °C) for culturing cell lines.

Real-time quantitative reverse transcription PCR

To validated the expression of *TOP2A*, *CDK1*, *Proliferating cell nuclear antigen (PCNA)*, and *ACTA2* in EPN cell lines and HEB cells, we conducted RT-qPCR applying FastStart Universal SYBR Green Master (ROX; Roche Diagnostics, Risch-Rotkreuz, Switzerland) in a CFX96 Real-Time System (Bio-Red Laboratories, Hercules, CA, USA) base on the manufacturer's instructions, and expression levels were normalized to glyceraldehyde-3-phosphate dehydrogenase (GAPDH). The $2^{-\Delta\Delta Ct}$ method was applied for RT-qPCR data analysis (13). The genes primers were: TOP2A sense, 5'-ACCATTGCAGCCTGTAAATGA-3'; TOP2A anti-sense, 5'-ACAGGATGAGGTACACTGGTTG-3'; CDK1 sense, 5'-AAACTACAGGTCAAGTGGTAGCC-3'; CDK1 anti-sense, 5'-TCCTGCATAAGCACATCCTGA-3'; PCNA sense, 5'-CCTGCTGGGATATTAGCTCCA-3'; PCNA anti-sense, 5'-CAGCGGTAGGTGTCGAAGC-3'; ACTA2 sense, 5'-AAAAGACAGCTACGTGGGTGA-3'; ACTA2 anti-sense, 5'-GCCATGTTCTATCGGGTACTTC-3'; GAPDH sense, 5'-GGAGCGAGATCCCTCCAAAAT-3'; GAPDH anti-sense, 5'-GGCTGTTGTCATACTTCTCATGG-3'.

Clinical patient datasets for analysis

Expression datasets of genes were selected based on the Chinese Glioma Genome Atlas (CGGA; http://www.cgga.org.cn), the EPN samples, provides RNA sequencing data, comes from 325 patients (203 males and 122 females; age range, 8–81 years). We put all statistics into SPSS 22.0 for analysis. According to the expression of *TOP2A*, *CDK1*, *PCNA*, and *ACTA2*, patients were categorized into high- and lowexpressed groups. Subsequently, survival analysis was operated. We defined the prognostic outcome of EPN patients with progress-free (PFS) and overall (OS). This study considers $p<0.05$ as a significant difference.

RESULTS

Identification of DEGs

Of 12,392 DEGs identified in group GSE86574, 5983 were down- and 6409 upregulated, compared with 1909 and 1441, respectively, of 3350 DEGs identified from group GSE74195; 2918, and 2663 were down- and upregulated, respectively, in 5581 DEGs of GSE66354, and 3021, and 2700 were down- and upregulated, respectively, in 5721 DEGs of GSE50161. Figures 2A-E showed the heat map regarding hub genes of EPN and the Venn plot of DEGs. The Venn plot reveals 1462 common DEGs among the four groups. Details of Venn analysis showed in Supplemental Table I.

Enrichment of Functions and Pathway of DEGs

The abnormal expression genes were put into DAVID for GO and KEGG analysis. Results showed that EPN demonstrated 30 functions and 10 pathways that were up- or down-regulated aberrantly (Table I, Figure 2F). GO analysis demonstrated that in biological processes (BP), the upregulated DEGs enriched in chemical synaptic transmission, neurotransmitter secretion, regulation of exocytosis, glutamate secretion, and nervous system development, while the downregulated DEGs enriched in extracellular matrix organization, cilium morphogenesis, and positive regulation of osteoblast differentiation, cilium assembly, and collagen fibril organization. The upregulated DEGs significantly enriched in molecular function (MF), including syntaxin-1 and ion channel binding, GABA-A receptor activity, and calcium ion and calmodulin binding. The downregulated DEGs enriched in protein binding, extracellular matrix (ECM) structural constituents, peptide antigen binding, MHC class II receptor activity, and integrin binding. In addition, analysis of cell component (CC) implied that the upregulated DEGs enriched in cell junction, postsynaptic membrane, synapse, postsynaptic density, and plasma membrane, and the downregulated DEGs enriched in extracellular exosome, ECM, focal adhesion, endoplasmic reticulum lumen, and the integral component of lumenal side of endoplasmic reticulum membrane. Table I also demonstrates the most significant enriched pathways of the DEGs analyzed by KEGG analysis. Upregulated DEGs were enriched in retrograde endocannabinoid signaling, glutamatergic and GABAergic synapses, morphine addiction, and synaptic vesicle cycle, while the downregulated DEGs were enriched in ECM-receptor interaction, viral myocarditis, graft-versus-host disease, allograft rejection, and the Hippo signaling pathway. GSEA analysis of EPN identified that Hedgehog and Notch signaling, and Mismatch repair (MMR) KEGG pathways were significantly abnormally regulated in EPN (Figure 2G).

Modules of PPI network

The DEGs with degrees >60 were selected as hub genes applying the STRING database. Subsequently, the genes selected were determined (Table II). Among these genes, TP53 possessed the highest nodes in EPN (158). Moreover, the top three significant modules were selected using MCODE: the No. 1 module had 55 nodes and 415 edges in all, compared with 62 and 360, respectively, for the No. 2 module, and 79 and 357, respectively, for the No. 3 module (Figure 3A). The genes belong to the top three modules were mostly involved with cell cycle, endocytosis, translesion synthesis, glutamatergic synapse, GABAergic synapse, spliceosome, protein digestion and absorption, focal adhesion, and collagen fibril organization (showed in Table III).

Confirmation of hub genes by RT-qPCR

To verify the expression of *TOP2A*, *CDK1*, *PCNA*, and *ACTA2* in HEB and EPN cells (BXD-1425EPN, DKFZ-EP1NS, and R254), RT-qPCR was performed. Those genes expressed higher in EPN cell lines than HEB cells significantly (Figure 3B; all $p<0.05$; precise P-values are shown in Supplemental Table II). Moreover, the expression levels of genes *TOP2A*, *CDK1*, *PCNA*, and *ACTA2* were slightly different among those EPN cell lines.

Survival curve analysis of four hub genes

Survival curve analysis was conduct to clear the connection between prognosis of EPN patients and expression levels of TOP2A, CDK1, PCNA and ACTA2. The TOP2A low-expression patients have greater percent survival than TOP2A high-

Table I: Functional and Pathway Enrichment Analysis of Up-Regulated and Down-Regulated Genes in EPN

Expression	Category	Term	Count	%	p-value
Up-regulated	GOTERM_BP_DIRECT	GO:0007268~chemical synaptic transmission	53	8.03	3.77E-28
	GOTERM_BP_DIRECT	GO:0007269~neurotransmitter secretion	22	3.33	2.06E-18
	GOTERM_BP_DIRECT	GO:0017157~regulation of exocytosis	13	1.97	8.79E-12
	GOTERM_BP_DIRECT	GO:0014047~glutamate secretion	13	1.97	2.61E-11
	GOTERM_BP_DIRECT	GO:0007399~nervous system development	32	4.85	6.07E-09
	GOTERM_CC_DIRECT	GO:0030054~cell junction	83	12.58	6.09E-38
	GOTERM_CC_DIRECT	GO:0045211~postsynaptic membrane	43	6.52	1.14E-21
	GOTERM_CC_DIRECT	GO:0045202~synapse	40	6.06	1.66E-21
	GOTERM_CC_DIRECT	GO:0014069~postsynaptic density	38	5.76	2.17E-19
	GOTERM_CC_DIRECT	GO:0005886~plasma membrane	216	32.73	4.96E-15
	GOTERM_MF_DIRECT	GO:0017075~syntaxin-1 binding	10	1.52	1.19E-09
	GOTERM_MF_DIRECT	GO:0044325~ion channel binding	20	3.03	2.79E-09
	GOTERM_MF_DIRECT	GO:0004890~GABA-A receptor activity	8	1.21	1.16E-06
	GOTERM_MF_DIRECT	GO:0005509~calcium ion binding	48	7.27	2.31E-06
	GOTERM_MF_DIRECT	GO:0005516~calmodulin binding	21	3.18	2.71E-06
	KEGG_PATHWAY	hsa04723:Retrograde endocannabinoid signaling	27	4.09	5.15E-17
	KEGG_PATHWAY	hsa04724:Glutamatergic synapse	27	4.09	1.37E-15
	KEGG_PATHWAY	hsa04727:GABAergic synapse	23	3.48	1.42E-14
	KEGG_PATHWAY	hsa05032:Morphine addiction	23	3.48	6.62E-14
	KEGG_PATHWAY	hsa04721:Synaptic vesicle cycle	18	2.73	7.63E-12
Down-regulated	GOTERM_BP_DIRECT	GO:0030198~extracellular matrix organization	37	4.75	1.53E-14
	GOTERM_BP_DIRECT	GO:0060271~cilium morphogenesis	27	3.47	2.81E-11
	GOTERM_BP_DIRECT	GO:0045669~positive regulation of osteoblast differentiation	15	1.93	7.86E-08
	GOTERM_BP_DIRECT	GO:0042384~cilium assembly	21	2.70	1.09E-07
	GOTERM_BP_DIRECT	GO:0030199~collagen fibril organization	12	1.54	2.45E-07
	GOTERM_CC_DIRECT	GO:0070062~extracellular exosome	188	24.13	1.77E-14
	GOTERM_CC_DIRECT	GO:0031012~extracellular matrix	43	5.52	3.82E-13
	GOTERM_CC_DIRECT	GO:0005925~focal adhesion	46	5.91	8.36E-11
	GOTERM_CC_DIRECT	GO:0005788~endoplasmic reticulum lumen	30	3.85	3.91E-10
	GOTERM_CC_DIRECT	GO:0071556~integral component of lumenal side of endoplasmic reticulum membrane	11	1.41	7.84E-08
	GOTERM_MF_DIRECT	GO:0005515~protein binding	452	58.02	1.41E-17
	GOTERM_MF_DIRECT	GO:0005201~extracellular matrix structural constituent	16	2.05	3.76E-08
	GOTERM_MF_DIRECT	GO:0042605~peptide antigen binding	9	1.16	8.58E-06
	GOTERM_MF_DIRECT	GO:0032395~MHC class II receptor activity	7	0.90	1.35E-05
	GOTERM_MF_DIRECT	GO:0005178~integrin binding	16	2.05	1.51E-05
	KEGG_PATHWAY	hsa04512:ECM-receptor interaction	20	2.57	7.17E-09
	KEGG_PATHWAY	hsa05416:Viral myocarditis	14	1.80	1.06E-06
	KEGG_PATHWAY	hsa05332:Graft-versus-host disease	11	1.41	1.15E-06
	KEGG_PATHWAY	hsa05330:Allograft rejection	11	1.41	3.68E-06
	KEGG_PATHWAY	hsa04390:Hippo signaling pathway	22	2.82	3.74E-06

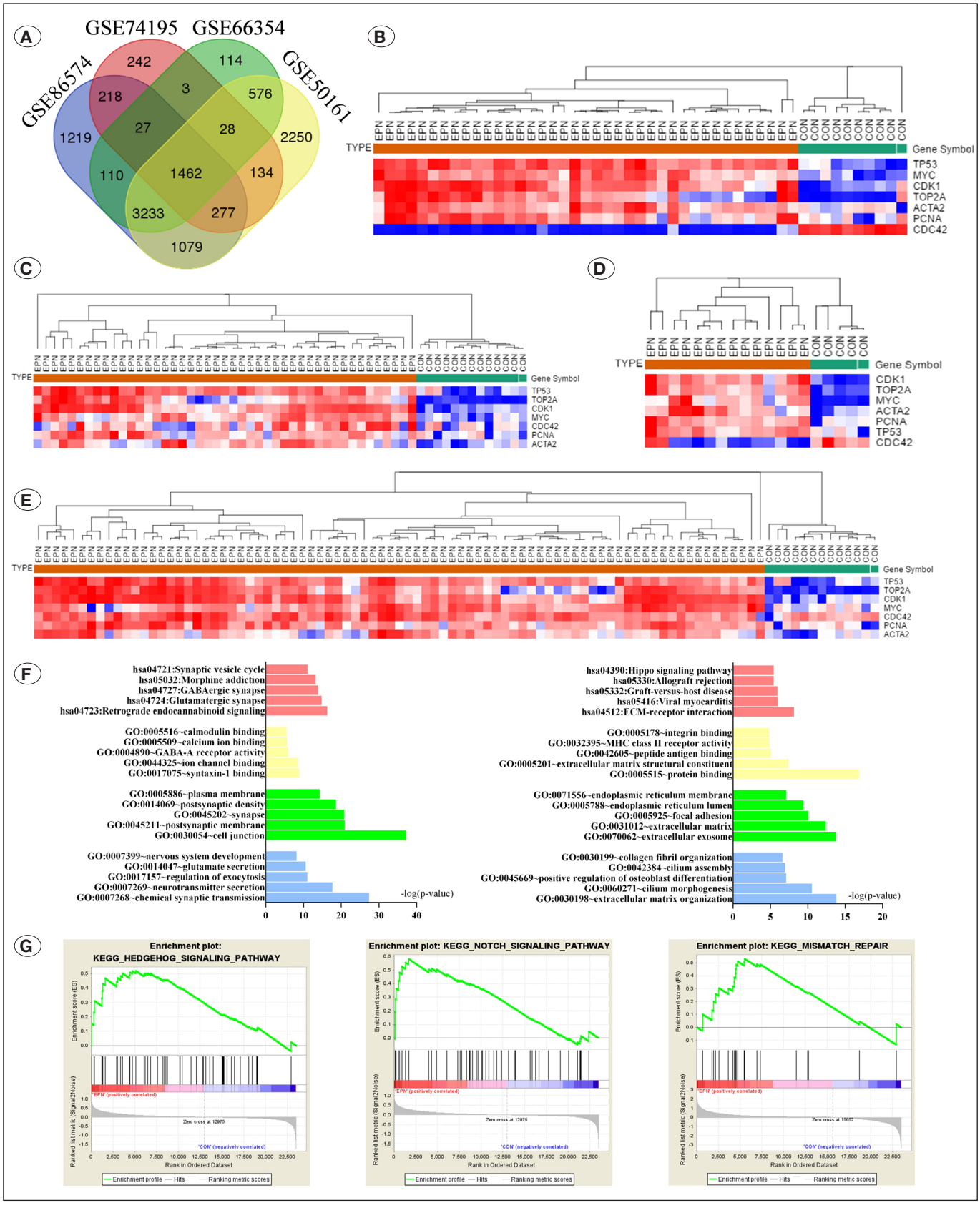

Figure 2: A) Functional and pathway enrichment analysis of up- and downregulated genes among four datasets. **B-E)** Hub gene expression heat map of four datasets. **F)** Venn plot of DEGs among three datasets. **G)** GSEA analysis results.

Table II: Key Nodes in the Protein-Protein Interaction Network With Degrees > 60(EPN)

Gene Symbol	Degree	Betweenness
TP53	158	0.111474
TOP2A	123	0.055364
CDK1	103	0.037421
PCNA	99	0.042523
ACTA2	98	0.049124
MYC	88	0.024017
UMPS	82	0.030001
CDC42	81	0.04123
NOTCH1	75	0.025682
CDK2	74	0.013782
PIK3CB	69	0.021616
ENO2	67	0.024474
PRKACB	66	0.026454
CDC20	66	0.01385
PAICS	65	0.012604
HDAC1	64	0.023285
KIF11	63	0.008449
ABL1	63	0.017247
CCND1	62	0.01233
ITGB1	62	0.023297

expression patients (PFS hazard ratio [HR] = 0.3402; 95% confidence interval [CI], 0.2541–0.4555; p<0.0001 and OS HR = 0.3904; 95% CI, 0.2925–0.5209; p<0.0001). CDK1 high-expression patients showed a worse percent survival compared with patients of CDK1 low-expression (PFS HR = 0.3232; 95% CI. 0.2411–0.4334, p<0.0001 and OS HR = 0.3321; 95% CI, 0.2464–0.4477, p<0.0001). The prognosis of *PCNA* high-expression sufferers obviously showed worse than that of *PCNA* low-expression sufferers regarding percent survival (PFS HR = 0.7400; 95% CI, 0.5603–0.9775, p=0.0331 and OS HR = 0.7033; 95% CI, 0.5286–0.9358, p=0.0313). *ACTA2* low-expression patients had a greater percent survival over *ACTA2* high-expression patients (PFS HR = 0.5967; 95% CI, 0.4513–0.7889; p<0.0001 and OS HR = 0.5627; 95% CI, 0.4223–0.7499, p<0.0001). That implied that a pleasant prognosis prefer patients with low expression of TOP2A, CDK1, PCNA and ACTA2 (p<0.05) (showed in Figure 4).

DISCUSSION

EPN, which accounts for 6.8% of all gliomas, is a common tumor occurs in brain with a relative frequency higher in children compared with its frequency in adults (4). Customary treatment includes surgery, subsequently followed by radiotherapy, but these always have resulted in a limited improved outcome (30). In addition, the recurrence rate of EPN is rather high. Thus, comprehending the etiological factors and molecular pathogenesis of EPN is critically vital for prevention, diagnosis, treatment, and prognosis of EPN. Microarray technology combining bioinformatics makes analysis of the genetic alteration and molecular mechanisms during the EPN formation process easy and convenient, and it should be used to provide a theoretical basis for targeted treatment of EPN (13).

Table III: Functional and Pathway Enrichment Analysis of the Modules Genes

Module	Term	Count	P Value	FDR	Genes
module 1	cfa04110:Cell cycle	6	3.72E-05	0.034633614	CDK1, MAD2L1, PCNA, BUB1B, TTK, CDC20
	cfa04144:Endocytosis	7	1.07E-04	0.099771701	SH3GL3, DNM3, ARRB1, DNAJC6, DNM1, SH3GL2, AMPH
	GO:0019985~translesion synthesis	3	3.65E-04	0.486721579	DTL, KIAA0101, PCNA
module 2	cfa04724:Glutamatergic synapse	11	1.43E-10	1.53E-07	GRM4, ADCY1, GRM3, PLCB4, GNG13, GNB5, GNG11, GNG3, GNG12, GNG5, GRM1
	cfa04727:GABAergic synapse	9	9.40E-09	1.01E-05	ADCY1, GABBR1, GNG13, GNB5, GNG11, GABBR2, GNG3, GNG12, GNG5
	cfa03040:Spliceosome	10	1.15E-08	1.23E-05	EIF4A3, SNRPD3, LSM7, ALYREF, LSM5, HNRNPC, SNRPF, SNRPE, PUF60, SNRPG
module 3	cfa04974:Protein digestion and absorption	11	2.54E-12	2.86E-09	COL4A2, COL9A2, COL4A1, COL3A1, COL6A2, COL1A2, COL6A1, COL1A1, COL5A2, COL5A1, COL4A5
	cfa04510:Focal adhesion	14	2.86E-12	3.22E-09	CDC42, CCND1, COL4A2, COL4A1, PIK3CB, ERBB2, COL3A1, COL1A2, COL6A2, COL6A1, COL1A1, COL5A2, COL5A1, COL4A5
	GO:0030199~collagen fibril organization	8	9.21E-12	1.30E-08	P4HA1, PLOD3, COL3A1, COL1A2, COL1A1, COL5A2, SERPINH1, COL5A1

We extracted data from GSE50161, GSE66354, GSE74195, and GSE86574 datasets containing gene expression profiles of both EPN and normal tissues, and identified a total of 5721 DEGs in GSE50161, 5581 in GSE66354, 3350 in GSE74195, and 12,392 in GSE86574. There were 1462 mutual DEGs among the four datasets. These DEGs were expressed were expressed abnormally which was significant. They apparently had important roles during the pathogenesis of EPN, and they might be applied as markers of diagnostic, treatment, and prognostic clinically.

The connection of DEGs was clarified applying GO and KEGG analysis, results pointed that DEGs located in this study mainly enriched in mitotic division, cell cycle, and microtubule and chromosome activities, which suggested the division of abnormal cell proliferation in EPN (25). Moreover, GO analysis results implied that the function of intercellular neurotransmitter delivery was abnormally regulated, which might be the reason for EPN often being complicated with cramps or epilepsy. Furthermore, MF and CC analysis results showed that the EPN cell patterns were totally different from those of normal cells, which suggests that EPN had more powerful cellular mechanisms to absorb more protein and inorganic salt and so forth, and to produce less protein on its surface that could be recognized as antigen. These changes in cyto-architectonics enabled a reduced probability of EPN to be detected by the

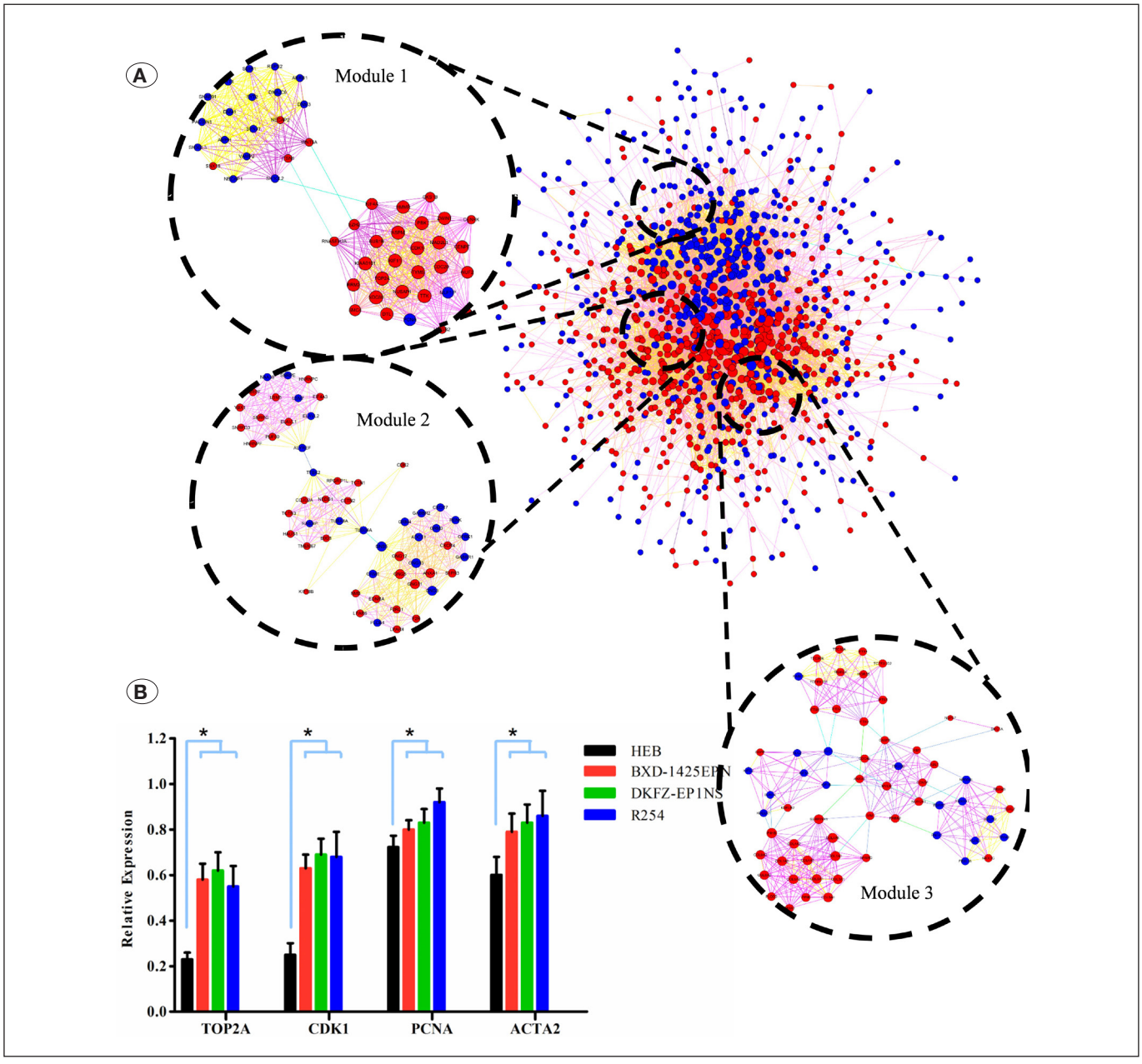

Figure 3: A) Top three modules from the PPI network. **B)** RT-qPCR validation of *TOP2A*, *CDK1*, *PCNA*, and *ACTA2* expression alterations *in vitro*. ***$p<0.05$.

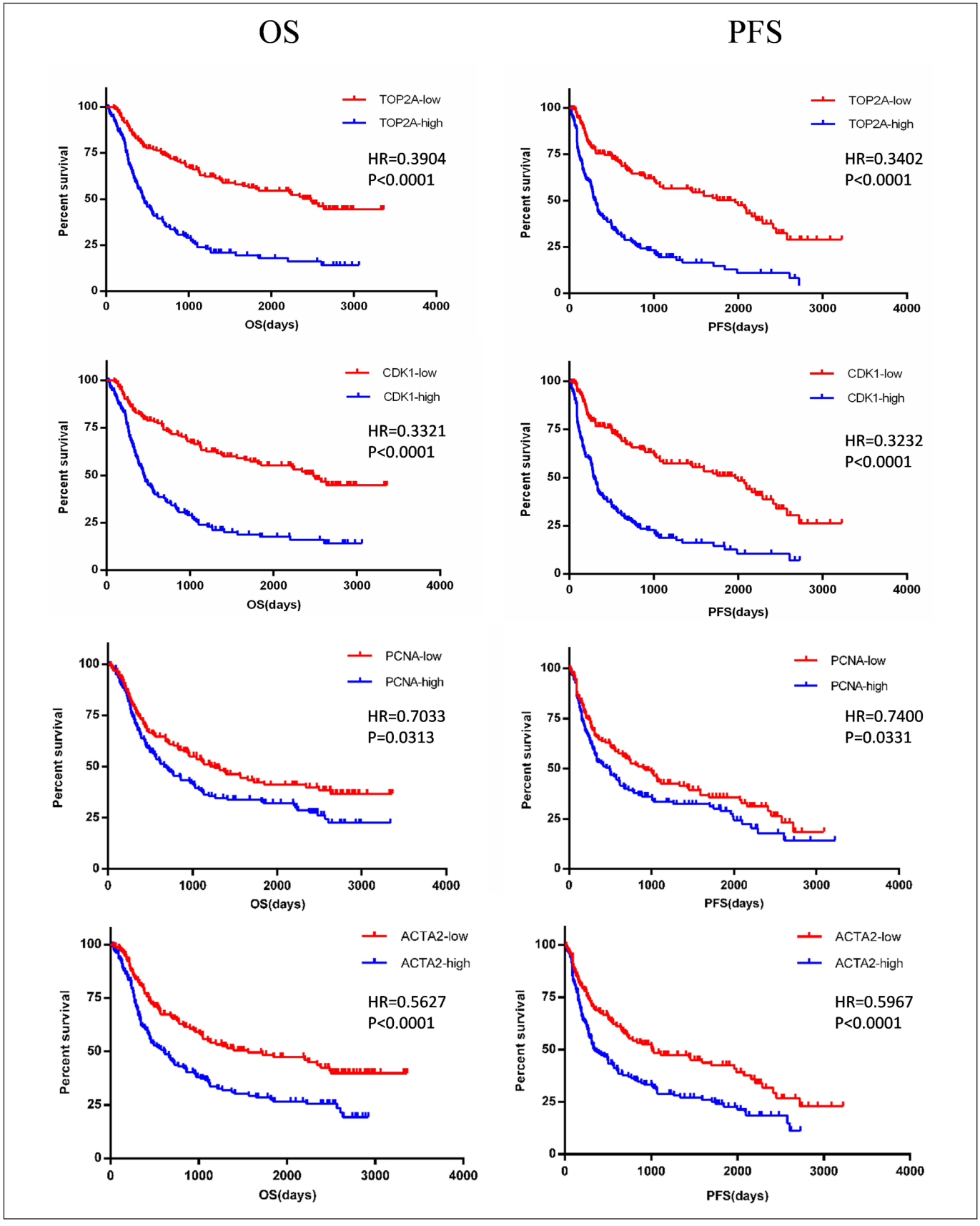

Figure 4: Survival curve analysis about common hub genes among four groups.

immune system, so that a better proliferative environment was provided for EPN.

The KEGG pathways mainly enrich in retrograde endocannabinoid signaling and morphine addiction. In the brain, endocannabinoids and cannabinoids combined with CB1 cannabinoid receptors on axon terminals and regulated the activities of ion channels and neurotransmitter release (21). Recent studies have also revealed that the endocannabinoid systems are closely related to a variety of cancers (8). It has been proven that abuse of morphine could up-regulate the expression of cannabinoid receptor, and obstructed normal functions of immune such as up-regulation of IL-4, IgG and IgM. That might increase tumor occurrence (36). Therefore, we suggested that retrograde endocannabinoid and morphine addiction might induce EPN formation. In our study, GSEA analysis showed that Hedgehog and Notch signaling and MMR had close connections with EPN, and that Hedgehog signaling contributed to cell growth and differentiation during embryogenesis and tissue homeostasis, as well as working in tumorigenesis. Hedgehog signaling had an active role in neuro-oncology diseases (1). Besides, latest studies pointed that Notch signaling had a fundamental role during development of astrocytic glioma and medulloblastoma, and that dysregulation of Notch signaling contributed to the malignant potential of these tumors (27). In addition, some studies have proved that patients with the biallelic lack of MMR genes would have a higher possibility of development of bone marrow, bowel, and brain tumors (34). Based on the aforementioned facts and our results, we thought that Hedgehog and Notch signaling, and MMR were important molecular foundations for the neoplastic processes of EPN, and they could be applied as diagnostic indicators, therapeutic targets, and prognostic biomarkers.

PPI network was performed applying both the STRING database and Cytoscape, and the DEGs with hub nodes >60 were selected as hub genes. The top seven genes, including TP53, *TOP2A*, *CDK1*, *PCNA*, and *ACTA2*, have much more degrees than others. *TP53*, tumor protein p53, encodes a protein that restrains tumor including transcriptional activation, DNA binding, and oligomerization domains. This encoded protain react to various cellular stresses and induces cell cycle arrest, apoptosis, senescence, or DNA repair by regulating expresssion of target genes. Lots of human cancer had been reported related to *TP53* mutations. Especially in brain tumors, the mutation of *TP53* both accelerate tumorigenesis as an early event, and progression to malignancy as a late event (20, 26). In our study, *TP53* obviously showed abnormal expression, so we emphasized its significance in EPN, and its mutations may be the key to the progression of EPN.

TOP2A (DNA topoisomerase II α) regulates and influences the topologic states of DNA during transcription, which plays roles in chromosome condensation, chromatid separation, and the relief of torsional stress that occurs during DNA transcription and replication. Several anticancer agents have been used targeting this gene, and the development of drug resistance was reported related to the mutations of TOP2A. Clinical studies have proved that eukaryotic type II topoisomerases (Top2α and Top2β) are important in alteration of DNA topology during the formation of normally-transient double strand DNA cleavage. Meanwhile, clinical patient survival data has revealed that *TOP2A* overexpression in primary tumors hints at more aggressive disease. Furthermore, according to past studies, significant positive correlation was observed between *TOP2A* and the histone methyltransferase, *EZH2*. Proteins encoded by *EZH2* play vital roles in keeping the transcriptional repressive state of genes, and they especially have some important roles in the CNS. *EZH2* is vital during early development, and its dysregulation is heavily linked to oncogenesis, such as EPN (7,11).

Cyclin-dependent kinases (CDKs), including four CDKs (*CDK1*, *CDK2*, *CDK4*, and *CDK6*), are important conditioning agent of cell cycle progression (32). *CDK1*, also named CDC2, plays an indispensable role for G1/S and G2/M phase transitions of the eukaryotic cell cycle, as a catalytic subunit of M-phase promoting factor. Phosphorylation and dephosphorylation of proteins encoded by CDK1 is vital in regulating mitochondrial function, and, as a result, mitochondrial homeostasis and cell-cycle progression were improved (14). It reported the connection between the abnormal expression of *CDK1* and a variety of tumors, such as colorectal, breast, hepatocellular, and laryngeal squamous cell carcinomas, and so forth (2, 10). Considering the key cell-cycle regulation function for cell proliferation of this gene, small molecules that inhibited *CDK1* were found to be potential anti-EPN agents (6). Our study showed that this gene, which was the core of the interaction between multiple genes, had a pivotal position in EPN tissues.

PCNA encodes a type of homotrimer protein, helping to improve the processivity of leading strand synthesis during DNA replication, as a cofactor of DNA polymerase δ. This protein encoded by PCNA is ubiquitinated and related to the RAD6-dependent DNA repair pathway. Previous studies noted that *PCNA* is indispensable in regulating DNA synthesis, DNA replication, cell cycle progression, and DNA damage responses by recruiting this protein to chromatin (28). *PCNA* participates in many important cellular processes, which benefit the multiplication and growth of cancer cells (31). Thus, inbibition of PCNA could be a potential effective way for treatment of EPN patients, and abundant structural studies have provided doable blockade management regarding *PCNA* (5). Therefore, blocking this gene function might be a novel treatment option for EPN.

ACTA2 (actin, α2, smooth muscle, aorta) encodes one of six different actin proteins. This actin protein, as an α actin, is highly conserved and vital in skeletal muscle cell motility, structure, and integrity. This gene also is known to contribute to cell-generated mechanical tension and maintenance of cell shape and movement. Mutations in this gene will cause a variety of vascular diseases. Meanwhile, the decrease in actin filament leads to enhancement of plasma membrane fluidity and the change in cell property, causing cytoskeletal disorder, which is a main characteristic of cancer cells. Prior studies have proved that aortic aneurysm familial thoracic type 6 caused by defects in this gene. Its abnormal expression significantly affects invasion and metastasis in lung adenocarcinoma (12). It also has been proved that amplification of *ACTA2* is

associated significantly with synchronous brain metastasis. In tissues of EPN, the expression of *ACTA2* was overwhelming. The overwhelming expression of *ACTA2* strongly suggested that *ACTA2* might be a driver gene during the EPN formation process.

Previous studies have fully proved that *TP53* has a close relationship with the prognosis of glioma and other kinds of brain tumors. In our study, RT-qPCR revealed that *TOP2A*, *CDK1*, *PCNA*, and *ACTA2* expressed higher in EPN cell lines than HEB cells significantly ($p<0.05$). Besides, the connection between prognosis of EPN patients and expression levels of the genes selected (*TOP2A*, *CDK1*, *PCNA*, and *ACTA2*) also was cleared, which implied a pleasant prognosis regarding PFS and OS ($p<0.05$), with low expression of *TOP2A*, *CDK1*, *PCNA*, and *ACTA2*, which was initially reported. These results suggested a new way for prognosis prediction of EPN patients by determining the expression levels of *TOP2A*, *CDK1*, *PCNA*, and *ACTA2*. Furthermore, considering the extensive connection between these four hub genes and the DEGs in EPN, the prediction that drugs targeting genes identified in this study would get a promising therapeutic effect for EPN patients is reasonable. *MYC* and *CDC42* are also identified as hub genes of EPN; however, there is lack of experimental and prognostic verification. Therefore, we did not depict *MYC* and *CDC42* in detail.

In addition, recent studies have identified the *C11orf95-RELA* fusion gene as a driver factor during the EPN formation process. Through acting on the NF-κB, the *C11orf95-RELA* fusion gene interferes with normal immune reaction and apoptosis, which ultimately leads to EPN (3). Other studies also proved that *TOP2* affects NF-κB dependent transcription during osteoclast differentiation (24). Therefore, it is reasonable to hypothesize that *TOP2A* could be an efficient therapeutic and diagnostic target of *C11orf95-RELA* fusion-positive EPN. Other researchers through bioinformatics have also identified *H3F3A* and *ATRX* mutations as potential causes of EPN, and it has been proved that these two genes aberrantly regulate cell replication (19). Our study used similar, yet more complicated bioinformatics methods to reveal the hub genes and abnormal regulated signal pathways of EPN, which to our knowledge have not been reported previously.

However, some limitations remain in this study. To reach a solid conclusion need further correlative studies. The detailed mechanism must be investigated further in future studies. In addition, it was difficult to identify the heterogeneity among the EPNs growing at different locations in this study, since the number of EPN samples recording their growing locations was so limited, and results based on such few single-race samples are not convincing and solid. Studies must be conducted to identify and clarify the different characteristics and developing processes among the EPNs growing at various locations in the future.

CONCLUSION

The DEGs discovered in our research provided comprehensive and profound perception into the molecular mechanism and pathogenesis of EPN. *TP53*, *TOP2A*, *CDK1*, *PCNA*, and *ACTA2* are the hub genes of EPN development. Patients with lower expression of *TOP2A*, *CDK1*, *PCNA*, and *ACTA2* showed a favorable OS and PFS. *TOP2A*, *CDK1*, *PCNA*, and *ACTA2* could be used significantly for the prognosis prediction of EPN patients, also indicate a promising treatment effect applying targeted drugs. Hedgehog signaling, Notch signaling, and MMR were closely related to the neoplastic processes of EPN, which potentially could be applied as diagnostic indicators, therapeutic targets, and prognostic biomarkers.

ACKNOWLEDGEMENTS

This study was supported by grants from the National Natural Science Foundation of China (Nos. 21401072 and 81302173), the S&T Development Planning Program of Jilin Province (Nos. 20160101086JC, 20150520045JH, 20130206039SF and 20130522029JH) Bethune project of Jilin University (No.2013205022) and Jilin Province Natural Science Foundation Project (No.3D5153023428). We thanked Enago (www.enago.com) for the English language review.

For supplementary materials, please visit https://turkishneurosurgery.org.tr/abstract.php?id=2903

AUTHORSHIP CONTRIBUTION

The authors (SZ, QY, JG, GD, HX, GZ) confirm responsibility for the following: study conception and design, data collection, analysis and interpretation of results, and manuscript preparation.

REFERENCES

1. Abiria SA, Williams TV, Munden AL, Grover VK, Wallace A, Lundberg CJ, Valadez JG, Cooper MK: Expression of Hedgehog ligand and signal transduction components in mutually distinct isocitrate dehydrogenase mutant glioma cells supports a role for paracrine signaling. J Neurooncol 119:243-251, 2014
2. Bednarek K, Kiwerska K, Szaumkessel M, Bodnar M, Kostrzewska-Poczekaj M, Marszalek A, Janiszewska J, Bartochowska A, Jackowska J, Wierzbicka M, Grenman R, Szyfter K, Giefing M, Jarmuz-Szymczak M: Recurrent CDK1 overexpression in laryngeal squamous cell carcinoma. Tumour Biol 37:11115-11126, 2016
3. Gessi M, Giagnacovo M, Modena P, Elefante G, Gianno F, Buttarelli FR, Arcella A, Donofrio V, Diomedi Camassei F, Nozza P, Morra I, Massimino M, Pollo B, Giangaspero F, Antonelli M: Role of immunohistochemistry in the identification of supratentorial C11ORF95-RELA fused ependymoma in routine neuropathology. Am J Surg Pathol 2017 (Epub ahead of print)
4. Goldwein JW, Leahy JM, Packer RJ, Sutton LN, Curran WJ, Rorke LB, Schut L, Littman PS, D'Angio GJ: Intracranial ependymomas in children. Int J Radiat Oncol Biol Phys 19:1497-1502, 1990
5. Gravells P, Tomita K, Booth A, Poznansky J, Porter AC: Chemical genetic analyses of quantitative changes in Cdk1 activity during the human cell cycle. Hum Mol Genet 22:2842-2851, 2013
6. Griesinger AM, Witt DA, Grob ST, Georgio Westover SR, Donson AM, Sanford B, Mulcahy Levy JM, Wong R, Moreira DC, DeSisto JA, Balakrishnan I, Hoffman LM, Handler MH,

Jones KL, Vibhakar R, Venkataraman S, Foreman NK: NF-kappaB upregulation through epigenetic silencing of LDOC1 drives tumor biology and specific immunophenotype in Group A ependymoma. Neuro Oncol 19:1350-1360, 2017

7. Gu L, Smith S, Li C, Hickey RJ, Stark JM, Fields GB, Lang WH, Sandoval JA, Malkas LH: A PCNA-derived cell permeable peptide selectively inhibits neuroblastoma cell growth. PLoS One 9:e94773, 2014
8. Han Li C, Chen Y: Targeting EZH2 for cancer therapy: Progress and perspective. Curr Protein Pept Sci 16:559-570, 2015
9. Huang K, Sun J, Yang C, Wang Y, Zhou B, Kang C, Han L, Wang Q: HOTAIR upregulates an 18-gene cell cycle-related mRNA network in glioma. Int J Oncol 2017 (Epub ahead of print)
10. Kim SJ, Nakayama S, Shimazu K, Tamaki Y, Akazawa K, Tsukamoto F, Torikoshi Y, Matsushima T, Shibayama M, Ishihara H, Noguchi S: Recurrence risk score based on the specific activity of CDK1 and CDK2 predicts response to neoadjuvant paclitaxel followed by 5-fluorouracil, epirubicin and cyclophosphamide in breast cancers. Ann Oncol 23:891-897, 2012
11. Kirk JS, Schaarschuch K, Dalimov Z, Lasorsa E, Ku S, Ramakrishnan S, Hu Q, Azabdaftari G, Wang J, Pili R, Ellis L: Top2a identifies and provides epigenetic rationale for novel combination therapeutic strategies for aggressive prostate cancer. Oncotarget 6:3136-3146, 2015
12. Lee HW, Park YM, Lee SJ, Cho HJ, Kim DH, Lee JI, Kang MS, Seol HJ, Shim YM, Nam DH, Kim HH, Joo KM: Alpha-smooth muscle actin (ACTA2) is required for metastatic potential of human lung adenocarcinoma. Clin Cancer Res 19:5879-5889, 2013
13. Liang B, Li C, Zhao J: Identification of key pathways and genes in colorectal cancer using bioinformatics analysis. Med Oncol 33:111, 2016
14. Liu R, Fan M, Candas D, Qin L, Zhang X, Eldridge A, Zou JX, Zhang T, Juma S, Jin C, Li RF, Perks J, Sun LQ, Vaughan AT, Hai CX, Gius DR, Li JJ: CDK1-Mediated SIRT3 activation enhances mitochondrial function and tumor radioresistance. Mol Cancer Ther 14:2090-2102, 2015
15. Louis DN, Ohgaki H, Wiestler OD, Cavenee WK, Burger PC, Jouvet A, Scheithauer BW, Kleihues P: The 2007 WHO classification of tumours of the central nervous system. Acta Neuropathol 114:97-109, 2007
16. Louis DN, Perry A, Reifenberger G, von Deimling A, Figarella-Branger D, Cavenee WK, Ohgaki H, Wiestler OD, Kleihues P, Ellison DW: The 2016 World Health Organization Classification of Tumors of the Central Nervous System: A summary. Acta Neuropathol 131:803-820, 2016
17. Margolin-Miller Y, Yanichkin N, Shichrur K, Toledano H, Ohali A, Tzaridis T, Michowitz S, Fichman-Horn S, Feinmesser M, Pfister SM, Witt H, Tabori U, Bouffet E, Ramaswamy V, Hawkins C, Taylor MD, Yaniv I, Avigad S: Prognostic relevance of miR-124-3p and its target TP53INP1 in pediatric ependymoma. Genes Chromosomes Cancer 56:639-650, 2017
18. Nieder C, Andratschke NH, Grosu AL: Re-irradiation for recurrent primary brain tumors. Anticancer Res 36:4985-4995, 2016
19. Nobusawa S, Hirato J, Yokoo H: Molecular genetics of ependymomas and pediatric diffuse gliomas: A short review. Brain Tumor Pathol 31:229-233, 2014
20. Olivier M, Langerod A, Carrieri P, Bergh J, Klaar S, Eyfjord J, Theillet C, Rodriguez C, Lidereau R, Bieche I, Varley J, Bignon Y, Uhrhammer N, Winqvist R, Jukkola-Vuorinen A, Niederacher D, Kato S, Ishioka C, Hainaut P, Borresen-Dale AL: The clinical value of somatic TP53 gene mutations in 1,794 patients with breast cancer. Clin Cancer Res 12:1157-1167, 2006
21. Piomelli D: The molecular logic of endocannabinoid signalling. Nat Rev Neurosci 4:873-884, 2003
22. Prokopienko M, Kunert P, Podgorska A, Marchel A: Surgical treatment of intramedullary ependymomas. Neurol Neurochir Pol 51:439-445,2017
23. Ramaswamy V, Taylor MD: Treatment implications of posterior fossa ependymoma subgroups. Chin J Cancer 35:93, 2016
24. Robaszkiewicz A, Qu C, Wisnik E, Ploszaj T, Mirsaidi A, Kunze FA, Richards PJ, Cinelli P, Mbalaviele G, Hottiger MO: ARTD1 regulates osteoclastogenesis and bone homeostasis by dampening NF-kappaB-dependent transcription of IL-1beta. Sci Rep 6:21131, 2016
25. Sandberg AA, Chen Z: Cancer cytogenetics and molecular genetics: Detection and therapeutic strategy. In Vivo 8:807-818, 1994
26. Shiraishi S, Tada K, Nakamura H, Makino K, Kochi M, Saya H, Kuratsu J, Ushio Y: Influence of p53 mutations on prognosis of patients with glioblastoma. Cancer 95:249-257, 2002
27. Stockhausen MT, Kristoffersen K, Poulsen HS: Notch signaling and brain tumors. Adv Exp Med Biol 727:289-304, 2012
28. Strzalka W, Ziemienowicz A: Proliferating cell nuclear antigen (PCNA): A key factor in DNA replication and cell cycle regulation. Ann Bot 107:1127-1140, 2011
29. Teo C, Nakaji P, Symons P, Tobias V, Cohn R, Smee R: Ependymoma. Childs Nerv Syst 19:270-285, 2003
30. Vitanza NA, Partap S: Pediatric ependymoma. J Child Neurol 31:1354-1366, 2016
31. Wang G, Cao X, Lai S, Luo X, Feng Y, Xia X, Yen PM, Gong J, Hu J: PI3K stimulates DNA synthesis and cell-cycle progression via its p55PIK regulatory subunit interaction with PCNA. Mol Cancer Ther 12:2100-2109, 2013
32. Xi Q, Huang M, Wang Y, Zhong J, Liu R, Xu G, Jiang L, Wang J, Fang Z, Yang S: The expression of CDK1 is associated with proliferation and can be a prognostic factor in epithelial ovarian cancer. Tumour Biol 36:4939-4948, 2015
33. Xing Z, Ni Y, Zhao J, Ma X: Hydrogen peroxide-induced secreted frizzled-related protein 1 gene demethylation contributes to hydrogen peroxide-induced apoptosis in human U251 glioma cells. DNA Cell Biol 36:347-353, 2017
34. Yeung JT, Pollack IF, Shah S, Jaffe R, Nikiforova M, Jakacki RI: Optic pathway glioma as part of a constitutional mismatch-repair deficiency syndrome in a patient meeting the criteria for neurofibromatosis type 1. Pediatr Blood Cancer 60:137-139, 2013
35. Zhang C, Peng L, Zhang Y, Liu Z, Li W, Chen S, Li G: The identification of key genes and pathways in hepatocellular carcinoma by bioinformatics analysis of high-throughput data. Med Oncol 34:101, 2017
36. Zhang QY, Zhang M, Cao Y: Exposure to morphine affects the expression of endocannabinoid receptors and immune functions. J Neuroimmunol 247:52-58, 2012

SUPPLEMENTARY MATERIALS

Supplement Table I: Venn Plot Analysis Results of DEGs among Four Datasets

Total	Elements	Elements	Elements	Elements
1462	FSTL1	OLFML2A	MBD2	NAP1L5
	RALYL	ZCCHC12	KIF5C	ZHX2
	CXCR4	PPM1H	MAGI2-AS3	TAGLN3
	DECR1	FSTL5	ZC3H14	ENPEP
	PTPRR	PDAP1	PIFO	PVALB
	PXYLP1	EIF4E2	DPP6	PLEKHH1
	RTN1	RDX	SLC25A24	LPCAT4
	NR4A2	CELSR3	TCTN3	ABCC5
	WDR34	ITSN1	ATL1	ABL1
	COL1A1	CAMK2B	FAM153A /// FAM153B /// FAM153C /// LOC100507387 /// LOC101928349 /// LOC101930363	TSPYL1
	CA11	CADPS2		MOBP
	ALDOC	TMEM248		ZBBX
	NUDT1	SEMA3G	ANXA2	DCAF13
	PRDM2	SLC2A10	MCF2L	NME5
	KCNC1	KIF4A	TBC1D24	B3GALT6
	NEFH	WDR16	AMPH	RUNX2
	PGBD5	IPO4 /// TM9SF1	OBSL1	MBNL3
	SNRPN /// SNURF	BICD1	HEATR5A	ODC1
	SYT13	PLA2G4C	SLC35F5	TMEM218
	CETN3	ENKUR	CD276	ZNF204P
	CDK1	CASC10	CEND1	TRPM3
	HS2ST1	RAB11FIP4	TCEAL2	TMEM64
	PPM1A	SQLE	GFOD1	RAPGEF5
	CPEB3	NEGR1	CTNNA1	PPP4R2
	MLF1	FGF12	PFKFB2	SLC2A4RG
	ID1	CACNG2	PRMT5	ERMN
	PIK3CB	ELF1	PAK7	CHURC1
	FAXC	HPCAL4	CLIC4	KLC2
	CLCN4	TYMS	ANKH	HDAC1
	NCDN	SDK2	SLC8A2	OIP5-AS1
	GRIK2	SNCA	SNX18	TMEM232
	SLITRK4	ARHGAP26	KCNK9	ATP2B3
	GNG12	CPNE9	SLC25A4	KDELR2
	CNTN2	EPB41L3	CPXM1	SH3GL2
	CLEC4GP1	PROS1	MAPKAPK3	RPN2
	UNG	VAT1	ZFP36L1	CTSO
	GSTP1	SHANK3	GPR161	TTC9B
	FKBP4	CCDC14	EMC10	JPH1
	MAD2L1	KCTD2	PURA	EFR3A
	EIF4A3	AMER3	ERBB2	N4BP2L1
	LMO4	MAGI1	GLT8D1	SLIT2
	MOB1B	KIF1B		NCOA7

Table I: Cont.

Elements	Elements	Elements	Elements
ODF3B	ESYT3	GABRA2	APH1A
ZNF804A	FAT2	PPIB	TP53INP1
LOC401220	VSNL1	SLC26A11	TUBB6
BMP2K	SPICE1	LOC100507547 /// PRRT1	KCNQ2
RHOBTB1	N4BP2	LOC101928747 /// RBMX /// SNORD61	NTN1
TMOD3	IGFBP7	BRINP1	AP3M1
SYT4	GPR22	SULT4A1	RRM2
RCBTB2	NCEH1	ARRDC4	SPTB
YPEL2	GRIN2C	MTUS1	SNX30
NRXN2	ARMC8	LINC00461 /// MIR9-2	AEBP1
LBR	SLC7A14	FGF14	DNTTIP1
ST8SIA5	SMC1A	HMGB2	C19orf54
NMB	ENAH	HNRNPC	NFATC2
EPB41L4A	SYNE4	ISG15	RAB13
NID1	ATP1A3 /// LOC101927137	TMEM67	SLC12A5
ZBED3	CD58	PRKCE	NRIP3
POLI	TMEM8A	COL3A1	TMX1
CLHC1	SSR3	C1QTNF4	SAP30BP
ZNF248	LOC284219	BTBD3	PRMT3
IRF2BP2	SV2B	ARMC3	GPRASP1
RNF41	HECW2	TUBA4A	SYNPR
MSN	ZDHHC4	SPAG17	C1orf226
EPDR1	KCNJ9	CC2D2A	TSPAN6
DDOST	COL6A2	NIFK	MPP3
NOS1	ANKS1B	PTPRN2	WWTR1
SYNGR3	PLGLB1 /// PLGLB2	EPB41L4A-AS1	PPP1R16B
INTU	ATP5S	MIR6890 /// QARS	GAS7
EML1	TCTN1	NAP1L3	CTNNAL1
GJB6	CRISPLD1	USP31	SOWAHC
GALNT13	SPIN4	ID4	VANGL1
SPATA17	SEZ6L2	SOX5	ACSL6
MAGEE1	P2RX5-TAX1BP3 /// TAX1BP3	INA	LOC283070
PLTP	PLD5	RREB1	CUEDC1
CNTN4	OXR1	AXIN2	ZFHX3
RAP1GAP2	FBXW9	LSM5	DPY19L4
EZH2	CDK5R2	SRRM3	SCRIB
IDI2-AS1	MADD	AP1G2	FZD6
FZD2	ARRB1	ORMDL2	GRM4
MRAP2	KCNK1	PSAT1	SMIM15
ZNF117	RUNDC3B	PTPN21	DYX1C1
KIF18B	SCAMP5	MOK	ANK3
NEFM	TCTEX1D2	IQGAP1	GTF2IRD1
SYN1	CDCA7		IFT57

Table I: Cont.

Elements	Elements	Elements	Elements
PPFIA4	SERPING1	PLCXD3	PPP1R14B
LMNA	TPCN1	KCNAB1	GNG3
IGIP	LRRC4C	RBM3	COPE
PEG10	MZT1	GRM1	IQCE
USP6NL /// USP6NL-IT1	ERLIN2	ITGB8	OPCML
MAGED2	TMEM151B	GXYLT2	CEP85L
LINC00599 /// MIR124-1	C14orf132	CDR2L	RBBP8
PGD	HLA-DRA	GLCE	SCN1B
GAD1	DNAH12	KLF9	JADE2
FJX1	EDNRA	PCSK2	ZFYVE28
CELF4	EFHC1	6-Sep	CALN1
BTG3	FUCA2	TMEM178A	ZNF423
ATP2B1	PENK	NUF2	KCNJ3
WASF2	OPRK1	GYG2	MYCN
CAMK2N2	CD99	GNA13	NID2
ELAVL3	LYSMD2	CNKSR2	LSM8
8-Sep	PKIB	AGA	MRPS16
TRAPPC6B	AGTRAP	GABRA1	CNIH4
SPOCK1	FN1	LIX1L	MIR4745 /// PTBP1
APBA1	DHFR	WEE1	NSMCE1
PLCE1	ATP1A1	SSR4	SSR1
CNTNAP1	MIR7110 /// PDIA5	ARMC2	FBXL7
HSD17B10	FNDC3B /// LOC101928615	KCNJ12 /// KCNJ18 /// LOC100996843	MAPRE2
SH3BP4	GANAB	EEF1A2	GABRB3
AES	C1orf198	MIPEP	GPR85
GOT1	NEDD4L	GPR155	ADAMTS3
UNC5A	ITGB1	MTUS2	GLS
FRY	IFT43	CHGB	SEC11A
CCDC64	NAPB	DIAPH3	KIAA1024
DAD1	DSE	ADARB1	PLGRKT
BSN	RGS8	COL4A2	LOX
COL9A2	FAM81B	SLC1A6	SYPL1
PALLD	GNS	UBASH3B	UNC80
PDIA3	ENO2	NOL4	RPS27L
USP32P2	BMP7	ZNF365	IQSEC3
CLN5	CCDC90B	PPP3CB	NARR /// RAB34
TMEM63C	MAP1A	HLA-DQB1 /// HLA-DRB1 /// HLA-DRB3 /// HLA-DRB4 /// LOC100996809 /// LOC101060835	BAG4
HS3ST1	CHN2	ZNF493	CAT
CABP1	RUNX1T1	SPPL2A	GABRG2
EMP2	PGGT1B	NEUROD2	LYZ
SLC6A15	CDK4		OLFML3
RIN2	CCDC176		ELAVL1
DNM1	TNFRSF19		CNDP1

Table I: Cont.

Elements	Elements	Elements	Elements
STXBP1	CRLS1	SLC44A1	PACSIN1
PTGR2	KIAA1430	ZC3HAV1L	SNAP23
PPIC	TMEM45A	CNTNAP4	GSTK1
SOWAHA	MPP7	CHST14	HES6
XRCC5	FBN2	ZNF217	REEP5
WDR90	GEMIN8	IQCG	FGF9
STX1B	FRRS1L	LOC285812	SPG21
SPHKAP	NUP62CL	STK33	ANKFY1
RMST	CCDC74A /// CCDC74B	HAR1A	TET2
GABBR2	SLC2A3	ASPHD1	HK2
KCND2	GNG5	TRIM9	MDK
PIP5K1B	CPLX1	PRSS3	PRKD1
ATP8A2	CAMK2D	DNAJC12	DNPH1
AGBL5	FLNC	GLI3	BRSK2
LRRC57	RCAN2	SLC17A7	ETS1
NXT2	NECAP2	CMTM6	BCAS1
OLFM3	C15orf65	KCNK12	STEAP2
GALNT1	CACNA1A /// LOC100507353	RP2	TMEM231
TTLL5	DSG2	FANCF	RYR2
ETV1	DHX40	PBK	GRN
ADAM11	RAB26	RAPGEF4	PROM1
PPARGC1B	DLL1	RFXANK	C18orf42
SLC16A1	MAPT	PDE1A	WSCD2
SOX2	C1orf21	ENKD1	MGAT4A
COMT	EPB41L1	ANXA5	CATSPER2 /// CATSPER2P1 /// LOC101930343
USP27X	CPNE2	ELOVL4	CYP26B1
EYA2	GUCY1B3	CCDC8	GNB5
S1PR3	TMEM246	CASKIN1	PRKAR1B
CKAP4	DNALI1	TEF	TCF3
EFS	ZC3HAV1	SHF	MSH5-SAPCD1 /// SAPCD1
MCTP1	CKS1B	FAM60A	BACH1
WLS	KIAA1407	LHX1	DTL
IQGAP2	SNAP25	HLA-F	BEND6
PCP2	IFT22	SYT1	LPAR6
C17orf97	SGSM1	LOC283713 /// OTUD7A	MEG3
MICU3	RHNO1	GABARAPL1 /// GABARAPL3	MEST
RBFOX3	GAS2L3	COLCA2	CTNND1 /// TMX2-CTNND1
C16orf52 /// LOC101930115 /// VWA3A	KIAA1107	YPEL4	NEDD9
GOLM1	B4GALT6	ASPM	PITPNM3
NRP1	LOC100506844	SERPINH1	RIMS2
CCDC50	RAB33A	ACTL6B	NPTN
ILF2	SPATA6	RASGRP1	SNRPD3
CCDC142 /// MRPL53	LOC101930324 /// NSF	CFI	SCN8A

Table I: Cont.

Elements	Elements	Elements	Elements
TMEM145	LPAR4	SUMF1	NDST3
HSD17B8	PRKCB	KDELR1	ZMAT1
YAP1	HES1	NCSTN	CAPN2
YBX3	SRRM4	PARP4	MYT1L
KSR2	FAM73A	SLC16A2	LRRTM2
PFN1	ZNF385B	IGFBP2	TTLL9
HLA-DRB1 /// HLA-DRB4 /// LOC100996809	VAT1L	NOTCH2	RGS11
SS18L1	FBXO31	CHCHD5	IPCEF1
SPATA13	F2RL1	TMOD2	TMEM251
MORN2	ARL13B	NR1D2	PPP1R3E
GNG13	PLCL2	TRHDE	PWAR6
GEM	PXDN	PTPN4	SPATA18
NANOS1	LIMD1	LAMA1	CRIP2
TBC1D9	RSPH4A	CDH11	ELMO1
TTK	MTX1	NDC80	UNC13A
TGFBI	IGF2 /// INS-IGF2	CDS2	IFT88
FANK1	PRDX4	MYC	CACNB2
OGDHL	GLIS2	NRXN1	GNG11
SPINT2	FGF1	E2F7	TBC1D32
HSPG2	VPS25	BGN	CDK2
ANO6	LRRC48	LZTS3	RHOJ
MAD2L2	SEZ6	MAPK1IP1L	CFC1 /// CFC1B
LRRC3B	CENPU	PPP4R1	LOC728613
GRIA2	CMTM3	SEC61A1	SYBU
NUSAP1	KRT222	TWSG1	CAMTA2
TTC30A	MED14	ZMYND10	GAS1
DNAJC10	TPBG	ADAMTS6	PEG3
RIT2	LONRF2	PQLC3	SGSH
KRTCAP2	DUSP18	CRNDE	VCAN
FARP1	NMNAT2	MKKS	SGK494
C15orf27	PSMF1	ADCY1	NHS
BTG2	IDS	TP53I3	FBXL16
MTHFD2L	SFRP2	UBE2QL1	SHANK2
NAP1L2	KCNJ6	UCP2	MIR4647 /// SLC35B2
LOC157562	TMED7 /// TMED7-TICAM2	SYN2	PDIA6
GPSM2	SOX9	YBX1	LURAP1L
HIST1H4J	GPR158	GRM3	NREP
COL4A5	CELF5	GRAMD1B	CCDC71L
KCNK3	ATP2B2	RMND5A	ZNF37BP
XK	ELAVL2	KIAA0408	AJUBA
PHYHIP	DLGAP1	UNC119B	SV2A
IGSF3	ACAP3	HAUS1	HOOK1
TEAD1	LAMTOR3	KIAA0513	MIR6741 /// PYCR2
	RAB15	MESDC1	MVB12A

Table I: Cont.

Elements	Elements	Elements	Elements
LINC00998	SPAG16	AKR7A2	XPR1
CENPK	B3GNT9	FKBP10	DALRD3
MAPKBP1	DGKH	SRBD1	SRCIN1
C14orf142	TAGLN2	SLC1A2	NEK11
LRRC27	SLC16A7	VIM	CREB3L2
SUCLG2	MEIS3P1	LGALS3BP	CLUHP3
RNA45S5	DNAJA4	KIAA1244	PRKAA2
PTCHD1	PRTFDC1	GABRB2	PACRG
DOCK7	DRAXIN	LIN7A	LINC01128
ABCC8	KIF11	SVOP	GRB10
MIR7703 /// PSME2	SYNC	RUVBL1	LOC400043
STMN2	FAM102B	GPR176	OSTC
COL1A2	DCAF12	ITPR1	EZH1
LTBP3	IFFO2	PKP4	CACNB4
ANKRD34C	TMCC2	DDAH2	STX1A
HSBP1	TCF12	MRC2	HNRNPF
CHST3	SNRPF	GARNL3	PABPC1L
MAP3K9	BCL2L2	CDC42	CXorf57
ACKR3	SGIP1	COL4A3BP	SLITRK5
ZNF22	RNF144A	NEUROD1	SYT3
PSD3	ANTXR2	WBSCR17	BRI3
C15orf61	OLFM1	MAP7D2	HNRNPDL
HECW1	MAPK9	RIMKLB	FUT9
ZNF519	ZNF540	DBNDD2 /// SYS1 /// SYS1-DBNDD2	KIFC2
B3GNT5	GRSF1	MDM1	MYCBP2
RYK	ABCC4	CD9	OGFOD3
MDFIC	ZFP36L2	ALDH7A1	WDR35
MBNL2	MAGT1	CDC20	CA10
ZNF385D	DYRK2	C3orf80	CD63
ID3	PCLO	E2F5	LIMS1 /// LIMS3 /// LIMS3L
IQCK	ABTB2	PRUNE2	TOP2A
FAM43B	TSPYL2	LHFPL4	EHD3
PTK2B	CDH18	CCDC40	ALDH1A1
MFSD6	VANGL2	UTP23	DNAH9
CHSY1	TTLL7	PLOD3	ANK1
GPR83	ZBED5-AS1	GABRA6	PPM1L
EXT2	SPOCK3	SERF1A /// SERF1B	TNFRSF10B
MAP3K5	GSN	LRP10	DBN1
PDLIM7	GLB1L2	TSPAN5	TSEN34
FAM13A-AS1	DGKZ	CTGF	FBL
ARPP21	UNC79	MCCC2	KCNIP4
MXRA8	ANK2	PLSCR3 /// TMEM256-PLSCR3	LOXL3
AP1G2 /// JPH4	SH3GL3		DYNC1I1

Table I: Cont.

Elements	Elements	Elements	Elements
PPP4C	RBP1	NUP37	GALNT2
ARHGAP44	PRRT2	CDS1	TMEM185B
ERF	KIF3C	TSPYL4	STK3
MTCL1	RUNDC3A	PPFIA3	REPS2
BAZ1A	SCG5	LTBP1	IMPACT
ZDHHC14	KLHL3	MAPRE1	ITGA6
SOCS2	TRHDE-AS1	CPEB1	GAD2
NKAIN2	NOTCH1	TMEM14C	CCND1
GLRB	SNAP91	EZR	SMCO4
HLA-DMA	SMARCE1	POU6F1	RASSF9
CBY1	ZAK	AKNA	SURF4
PAICS	NPTXR	ARL6IP6	TPPP3
SYNJ1	DPYSL3	HLF	CALB2
MMD	TTC7B	ITPRIPL2	PTPN14
HLA-B	TOB1	TLE2	SNRPG
TCF7L2	CENPF	TIAM1	DDR1 /// MIR4640
CACYBP	DPCD	PXMP2	PRKACB
CSRP2	SNCB	FAM126B	RIMS1
DAP	WDR63	ALYREF	RCN1
CASC1	IFT52	SCN1A	ZWINT
RPGR	CRTAM	GABBR1	KIF9
GPR125	PAK1	WDR96	SHISA8
MEF2BNB	B9D1	YWHAH	C7orf73 /// LOC101930655
C1orf192	IGF2BP3	UMPS	VPS53
CAMKK2	RAB3IP	C1QTNF5 /// MFRP	TMEFF2
NES	HMGN1	DDX39A	RSPH3
POP5	PTPN20B	TTC30B	YES1
SREK1	PUF60	KCND3	CLIC1
MAK	IMPDH2	COL5A2	IGFBP5
PGLS	ZNF702P	RAB9B	ERGIC3
COL6A1	SIX5	CYB561	EPHB1
STMN4	KCNA1	KIT	RPH3A
ANKRD34A	RHOC	SVIP	SLC38A6
SPARC	PPP3CA	MAP7	TRIP6
COL5A1	SPTSSA	SCN4B	DKFZP761C1711
ADAM22	ALKBH2	ANTXR1	C9orf116
PPP1R18	NPC2	TEX9	LOC101060405 /// RRN3P3
UHRF1	TMEM98	BARD1	FAM111A
SCN2B	PPM1K	DGCR5	INPP5F
MEX3C	RBFOX1	FDX1	GPC4
SSBP1	PCDH7	ZNF627	PSMD9
PDIA4	ORAI3	WNT5A	NXN
PCNXL2	TRAM1	MIR7109 /// PISD	PRKCZ

Table I: Cont.

Elements	Elements	Elements	Elements
CKMT1A /// CKMT1B	LAMB2	RAB3C	LRIG3
IL17RD	SUCO	NXPH3	GABRB1
PCNXL4	DGKE	GPX7	FBLN1
STK36	ADAM17	ACTL6A	HLA-DPA1
ROMO1	CHRNA3	CRYM	RIMS3
PLCB4	NDRG4	PHACTR3	RNF112
AASS	ALG5	CKLF /// CKLF-CMTM1	GDAP1
RPGRIP1L	NRXN3	NMRK1	PCNA
MEX3A	TCTEX1D1	GLB1 /// TMPPE	RBBP4
NECAP1	PREPL	WDR54	RGS7
SMAD1	ASPHD2	DAB1	HMP19
MIR1204 /// PVT1	RABGAP1L	RTN4R	HLA-DQB1 /// HLA-DRB1 /// HLA-DRB4 /// HLA-DRB5 /// LOC100996809 /// LOC101060835
TTC8	MAPK8IP3	SYT2	SCGN
GABRD	MXD1	KCNA2	STXBP5
EMP3	RGS17	LGALS1	MAP6D1
SYNCRIP	PLEKHG1	SGPL1	KIF5A
CBX7	INPP4A	SWAP70	PSENEN
F2R	LRRC75A-AS1 /// SNORD49A /// SNORD49B /// SNORD65	ABCA1	MYO5A
HLA-G	ZMPSTE24	REST	CCSAP
RGL2	TMEM107	DYNLT1	LRRC34
MFAP2	GRIA4	CADM2	GABARAPL1
SPA17	KIAA0101	IDH2	WDR78
CAMK4	RGS7BP	PRKD3	SIN3A
ARSD	PLEKHA6	CASP8	DIRAS2
CPLX2	CYFIP2	ERAP1	LOC100289230
RB1	TMEM56	CCNG2	SLC24A2
GPX8	APRT	CNN3	CDKL2
FBXW7	C11orf70	JAG1	NEDD1
MINA	SYNGR1	FAM226A /// FAM226B	RAB36
RBFOX2	SMIM13	CACNA1B	FBN1
YIF1A	YPEL3	SMC4	SLC35F3
FBXO41 /// LOC101927826	VGLL4	TTBK2	INHBB
HAT1	BRWD1	CTXN1	PRRC1
TDRD6	PPIP5K1	RPL22L1	AIMP2
LOC102724884 /// LOC728613 /// PDCD6	VAMP2	4-Sep	AP3B2
P4HA1	MEF2D	DUSP26	LAMC1
COL4A1	CYBA	LITAF	EFHC2
ISOC1	ANXA1	GNB2L1 /// SNORD95 /// SNORD96A	MAST1
TMEM123	AFF1	MYT1	B3GALTL
TGIF1	HMG20B	HECTD4	GAR1
TP53	BAI3	EMP1	LINC00632
ATP6V1G2	TRIM23	TENM1	
	KDELC2	SNRPE	

Table I: Cont.

Elements	Elements	Elements	Elements
ISYNA1	C7orf57	PAIP2B	CERS2
LSM7	KIAA1456 /// LOC101927137	RNASEH2A	F11R
DNAJC6	PLXDC2	DUSP8 /// LOC101927562	TMEM254
TPD52	CAPRIN1	IFT81	ACTA2
PGM2	ATRAID	CHRD	FKBP9
TMBIM4	TTC28	PEX10	KLF10
VEZF1	HPCAL1	KLC1	FAM131B
DNM3	HOMER1	EFCAB2	PARD3B
HMGN5	SERPINB6	AKAP13	VPS13C
CBLN1	SCN2A	ACN9	LOC285147
PRKRIR	FAIM2	HMMR	ANXA4
COTL1	MSX1	HEY2	GAB1
TNC	ST8SIA3	CETN2	UEVLD
ELMOD1 /// LOC643923	MICAL2	UNC13C	JPH3
DOCK9	CELSR1	10-Sep	PXK
DLG2	TTC21A	NPTX1	FLNA
SOCS7	KIAA1467	TMEM258	G6PC3
ZYG11B	MOB1A	KIAA1804	MDH1B
NCKAP5	MFSD4	ADCK3	MAL2
RORA	TMCO1	SSX2IP	TUBB4A
PTPRD	BICC1	SOX11	NDRG3
CYP4X1	ADAP1	HIVEP3	DACT1
SGK223	NIPAL3	ABLIM3	ST18
OPTN	BUB1B	P4HB	
DGKG	COX7A1	SPATA33	

Supplement Table II: Exact p Values of t-Tests in RT-qPCR Assays

	TOP2A	CDK1	PCNA	ACTA2
BXD-1425EPN vs HEB	<0.001	<0.001	0.043	0.019
DKFZ-EP1NS vs HEB	<0.001	<0.001	0.027	0.015
R254 vs HEB	<0.001	<0.001	0.011	0.004

HEB is a kind of human glial cell line, and BXD-1425EPN, DKFZ-EP1NS, R254 are ependymoma cell lines.